

Non-invasive Assessment of Fibrosis and Inflammation in Rat Kidney Models with Diffusion-Weighted MRI

Lindsey Alexandra Crowe¹, Iris Friedli¹, Christian Vesin², Lena Berchtold³, Pierre-Yves Martin⁴, Sophie de Seigneux⁴, and Jean-Paul Vallée¹

¹Division of Radiology / Faculty of Medicine, Geneva University Hospital, Geneva, Switzerland, ²Division of Cell Physiology and Metabolism, Geneva University Hospital, Geneva, Switzerland, ³Division of General Internal Medicine, Geneva University Hospital, Geneva, Switzerland, ⁴Division of Nephrology, Geneva University Hospital, Geneva, Switzerland

Introduction: Chronic kidney disease (CKD), defined as kidney injury and/or loss of kidney function is a significant worldwide health problem. CKD is associated with the apparition of renal fibrosis, which is considered as one of the most predictive elements of its evolution. Currently, fibrosis is estimated by renal biopsy. By defining a new non-invasive technique to assess renal fibrosis using a non-contrast MRI protocol, the proposed protocol can be directly translated to the clinical practice to improve the care of CKD patients and decrease significantly the numbers of renal biopsies needed.

A pre-clinical study to evaluate the performance of Readout Segmentation Of Long Variable Echo Train (RESOLVE) diffusion weighted imaging in well-controlled experimental models of renal fibrosis, using the same clinical 3T MR system as for the patients, was proposed. We compare images with the classical EPI single shot sequence (ss-EPI). Phantom and volunteer developments have been presented previously¹ and this animal study serves to introduce renal pathology. Two published experimental studies reporting a correlation between ADC and renal fibrosis have been performed on a dedicated high field MR system^{2,3}, but the ability of a clinical 3T MR system to differentiate between different renal fibrosis grades was largely unknown. We therefore studied two experimental models of renal fibrosis.

Methods: 24 male wistar rats (Janvier, France), weighing 150-175g and aged two months at receipt, were used in this study. Ethical committee approval was obtained for the protocol and animals were kept in the institutions animal facility with free access to food and water.

For the severe animal model of unilateral ureteral obstruction (UO), a total of 16 rats (16 UO, 16 internal controls) were scanned after undergoing a surgical unilateral ureteral obstruction procedure. Animals were imaged and sacrificed at time points of 1, 2 and 3 weeks ligation. The model of moderate interstitial inflammatory nephritis with bovine serum albumin (BSA) protein-overload nephropathy included total of 8 rats (with external control due to nephrectomy). One week following left-sided nephrectomy, rats were randomly divided into a BSA and a control group, with 5 rats in the BSA group and 3 rats in the control group. Animals were imaged and sacrificed at 2 and 3 weeks after injection.

The MRI was carried out on a Siemens Magnetom Trio, a 'Tim system' 3T clinical scanner (Siemens AG, Erlangen, Germany) with the manufacturer's wrist coil. For morphologic evaluation, a coronal T1 gradient echo was performed followed by the read-out segmented 'RESOLVE' sequence synchronized to the respiration for diffusion-weighted imaging. The diffusion gradients were applied in 3 orthogonal directions with 10 b-values (0, 10, 20, 40, 60, 150, 300, 500, 700, 900 s/mm²). An optimised ss-EPI was compared. Diffusion images were 1.2x1.2x2.2mm resolution and with bandwidth maximized. Cortical ADC was measured from fitted ADC exponentials. Histological fibrosis quantification was performed using non-polarized Sirius Red staining. Morphometric analysis (automated fibrosis assessment) was performed using the Inmaris Software. Cellular infiltration was automatically quantified using nuclei counts on haematoxylin eosin staining with the software. Correlations (Pearson's) were carried out per group (with internal controls) due to staining variations. Box plots and one-way ANOVA with post-hoc Bonferroni (p<0.05 was taken as statistically significant) were used to assess statistical differences.

Results:

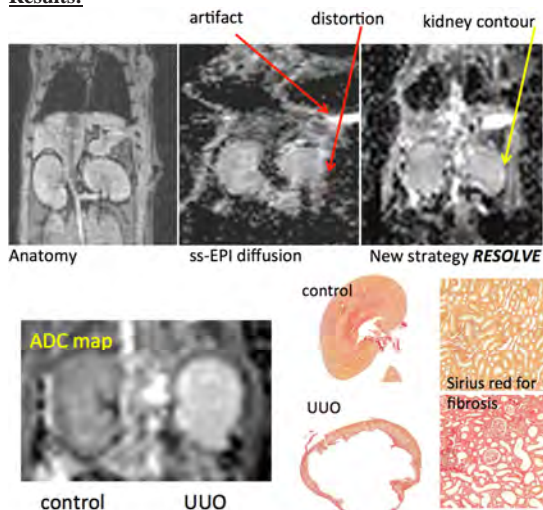


Figure 1. Translational study to test sequences with pathology. Image acquisition strategy in a rat model: Segmentation and high resolution = RESOLVE considerably limits the distortions that make standard diffusion images of non-exploitable.

Figure 2. 3T, Fibrosis and inflammation: Model of unilateral urinary obstruction (n = 16 with internal control). ADC map and histological slices of contralateral normal and UO kidney and zoom showing Sirius Red staining for fibrosis.

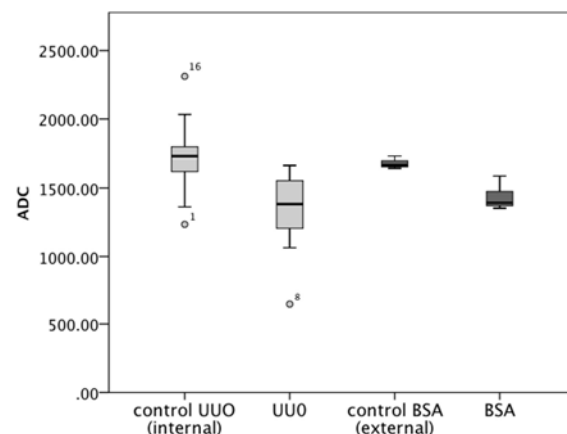


Figure 3. Difference in mean ADC (10⁶ mm²/s) between the control and models: UO at time points 1, 2 and 3 weeks and BSA at 3 weeks.

ss-EPI shows severe distortion, and 14% of kidneys could not be analysed for ADC. Uncertainty in region placement in the ss-EPI made further analysis difficult. A difference was still seen for the UO two-week group for example, but with a p value double that of RESOLVE. In the other groups tested n became too small with the non-analysed kidneys and in later experiments ss-EPI was not acquired due to the percentage of non-analysable images obtained. After full analysis from RESOLVE images, in both models ADC values showed a correlation with automated histological fibrosis assessment. In the UO model, a strong correlation was recorded overall between the ADC map values with the percentage of fibrosis (UO week 1, R²=0.6, week 2 R²=0.3, week 3 R²=0.7). For UO with cellular infiltration correlations were good at the later timepoints with more infiltration (UO week 1, R²=0.2, week 2 R²=0.5, week 3 R²=0.9). There was no correlation with cellular infiltration in the BSA model, but an R²=0.4 between ADC and fibrosis. The different timepoints of UO (1, 2 and 3 weeks) leads to a wider variation in ADC values shown in the box plot. However a significant difference is seen between internal control and UO (p<0.03) using grouped or individual timepoints. In the BSA model, less fibrosis was detectable in histology but a difference was still visible in the ADC values (p=0.007). This shows a low detection limit (sensitive method), even for fibrosis of <20%. The smaller BSA group showed less variability in the model and values and was also easier measurement of cortex due to the preserved kidney anatomy. Figure 3 shows this significant difference between groups in terms of ADC. In histology all groups showed a difference in fibrosis with controls and all UO a difference in cellular infiltration.

Discussion and Conclusions: These results overcome the challenge to measure diffusion in rodent on a clinical scanner. So far, a correlation between ADC and renal fibrosis in small animal was only observed on dedicated small animal systems operating at high field with gradient strength and field homogeneity much superior to any given clinical MR scanner. To confirm this correlation on a clinical 3T MR scanner was an important step in the translational research pathway going from observations on small animal to clinical applications. Our results demonstrated the power of the new RESOLVE strategy with histological validation, and are strong incentive to further apply RESOLVE to renal patients.

References

1. Friedli I, Crowe LA, Viallon M, et al. Improvement of Renal Diffusion-Weighted MR Imaging with Readout-Segmented Echo-Planar Imaging at 3T. Proc. Intl. Soc. Mag. Reson. Med. May 2014:2191.
2. Hueper K, Rong S, Gutberlet M, et al. T2 relaxation time and apparent diffusion coefficient for noninvasive assessment of renal pathology after acute kidney injury in mice: comparison with histopathology. Investigative radiology. Dec 2013;48(12):834-842.
3. Togao O, Doi S, Kuro-o M, et al. Assessment of renal fibrosis with diffusion-weighted MR imaging: study with murine model of unilateral ureteral obstruction. Radiology. Jun 2010;255(3):772-780.